

A Simple Method to Synthesize Cadmium Hydroxide Nanobelts

D. E. Zhang · X. D. Pan · H. Zhu · S. Z. Li · G. Y. Xu ·
X. B. Zhang · A. L. Ying · Z. W. Tong

Received: 6 May 2008 / Accepted: 11 July 2008 / Published online: 9 August 2008
© to the authors 2008

Abstract Cd(OH)₂ nanobelts have been synthesized in high yield by a convenient polyol method for the first time. XRD, XPS, FESEM, and TEM were used to characterize the product, which revealed that the product consisted of belt-like crystals about 40 nm in thickness and length up to several hundreds of micrometers. Studies found that the viscosity of the solvent has important influence on the morphology of the final products. The optical absorption spectrum indicates that the Cd(OH)₂ nanobelts have a direct band gap of 4.45 eV.

Keywords Crystal morphology · Nanobelt · Viscosity · Hydrothermal

Introduction

One-dimensional (1D) nanostructures such as wires, rods, belts, and tubes, whose lateral dimensions fall anywhere in the range of 1–100 nm, have become the focus of intensive research, owing to their unique applications in mesoscopic physics and fabrication of nanoscale devices [1–6]. Among one-dimensional (1D) nanostructures, nanobelts (or nanoribbons), a relatively new family of 1D nanostructures with a rectangular cross section, have received increasing attention

since the discovery of novel oxide semiconductor nanobelts [4–8]. A variety of functional oxide [3, 9] and sulfide [10–17] nanobelts have been successfully fabricated by simple thermal evaporation. The methods used in 1D nanostructure synthesis and hydrothermal processes have emerged as powerful tools for the fabrication of anisotropic nanomaterials with some significant advantages, such as controllable particle size and low-temperature, cost-effective, and less-complicated techniques. Under hydrothermal conditions, many starting materials can undergo quite unexpected reactions, which are often accompanied by the formation of nanoscopic morphologies that are not accessible by classical routes [18]. In recent years, 1D nanomaterials such as Ln(OH)₃ [19–21], CdWO₄ [22], MoO₃ [23], and Dy(OH)₃ [24] have been successfully synthesized using hydrothermal methods.

Cadmium hydroxide, Cd(OH)₂, is a wide band gap semiconductor [25] with a wide range of possible applications including solar cells, photo transistors and diodes, transparent electrodes, sensors, etc. [26, 27]. Cadmium hydroxide is also the precursor to prepare cadmium oxide [18]. As a consequence, numerous techniques have been proposed to synthesize nano-sized Cd(OH)₂ particles with promising control of properties [25–28]. However, up to now, to our best knowledge, the synthesis of Cd(OH)₂ nanobelts by hydrothermal process has not been reported. Herein, we report the preparation of cadmium hydroxide nanobelts by the conventional polyol assisted hydrothermal process.

Materials and Methods

In a typical procedure; CdCl₂ · 2H₂O (0.2281 g) was dissolved in 32 mL of distilled water, and then NH₃ · H₂O (25 wt.%, 5 mL) was slowly added into the solution and stirred for about 10 min, and a transparent Cd(NH₃)₄²⁻

D. E. Zhang (✉) · X. D. Pan · H. Zhu · S. Z. Li ·
G. Y. Xu · X. B. Zhang · A. L. Ying · Z. W. Tong
Department of Chemical Engineering, Huaihai Institute of
Technology, Lianyungang 222005, People's Republic of China
e-mail: zdewxm@yahoo.com.cn

Z. W. Tong (✉)
SORST, Japan Science and Technology Agency (JST), Tokyo,
Japan
e-mail: tong@hhit.edu.cn

solution was formed. Then, the above solution was loaded into a 50-mL Teflon-lined autoclave, which was then filled with 8 mL of glycol. The autoclave was sealed, warmed up at a speed of 3 °C/min and maintained at 100 °C for 6 h, and was then cooled to room temperature on standing. The white precipitate was filtered off, washed with absolute ethanol and distilled water for several times, and then dried in vacuum at 40 °C for 4 h.

X-ray diffraction (XRD) patterns were carried out on a Japan Rigaku D/max rA X-ray diffractometer equipped with graphite-monochromatized high-intensity Cu K α radiation ($\lambda = 1.541784 \text{ \AA}$). The accelerating voltage was set at 50 kV, with 100 mA flux at a scanning rate of 0.06°/s in the 2θ range 10–80°. The X-ray photoelectron spectra (XPS) were collected on an ESCALab MKII X-ray photoelectron spectrometer using nonmonochromatized Mg KR X-ray as the excitation source. The field emission scanning electron microscopy (FE-SEM) images were taken on a JEOL JSM-6700FSEM. The transmission electron microscopy (TEM) images were characterized by Hitachi H-800 transmission electron microscope with a tungsten filament and an accelerating voltage of 200 kV.

Results and Discussion

The XRD pattern (Fig. 1) from the as-synthesized bulk samples reveals the crystal structure and phase purity of the products. All the diffraction peaks can be indexed to the hexagonal Cd(OH) $_2$ with cell constants $a = 3.4942$, $c = 4.7102$, which are consistent with the values in the literature (JCPDS 31-0228). The abnormally intensified (100) peak in the XRD pattern also indicates that the belt-

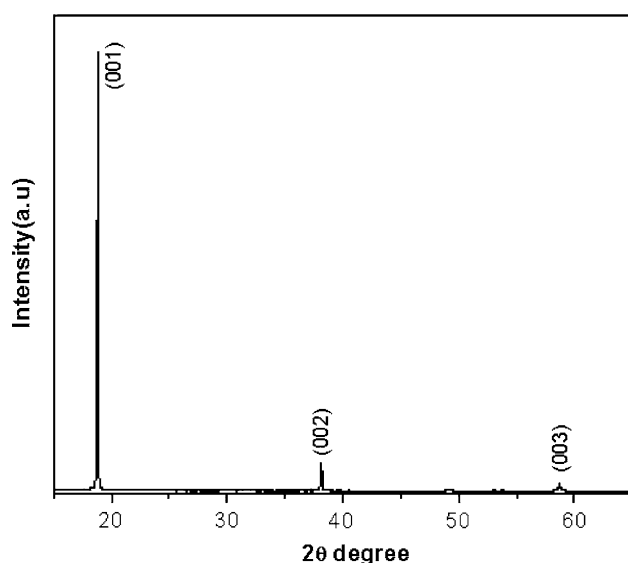


Fig. 1 Powder XRD patterns of the products

like product comprises 1D Cd(OH) $_2$ crystals preferentially grown along the [001] direction.

Figure 2 shows the XPS spectra of the as-obtained Cd(OH) $_2$ sample. A survey spectrum shown in Fig. 2a, indicates the presence of Cd and O as well as C from reference. There are no peaks for other impurities, indicating that the as-obtained product is relatively pure. High-resolution spectra are also taken for the Cd 3d region and the O 1s region to determine the valency state and atomic ratio. The binding energies of Cd(3d $_{5/2}$) and O(1s) were found to be 405.30 and 531.25 eV, respectively. All the above observed binding energy values are in good agreement with the reported data [29, 30]. Quantification of the XPS peaks gives the molar ratio of Cd:O as 1:2.02, close to the stoichiometry of Cd(OH) $_2$. This also validated our speculation in XRD study.

A typical low-magnification FESEM image (Fig. 3a) shows that the as-synthesized products consist of a large quantity of 1D nanostructures with lengths from several tens to several hundreds of micrometers; some of them even have lengths of the order of millimeters. A representative high magnification SEM image (Fig. 3b) of several curved Cd(OH) $_2$ 1D nanostructures reveals that their geometrical shape is belt-like, which is distinct from those of previously reported nanowires, and their thickness is about 30–50 nm.

TEM and SAED studies of the as-synthesized products provide further insight into the belt-like Cd(OH) $_2$ nanostructures. Straight and curved Cd(OH) $_2$ nanobelts can be observed in Fig. 4b. The nanobelts are uniform in width and thickness, and their typical widths and thickness are in the range of 60–250 nm and 10–30 nm, respectively. The SAED pattern (inset in Fig. 4b) taken from the straight section of the curved nanobelt demonstrates that this particular nanobelt is a single crystal.

For the polyol process, glycol was selected as the solvent because of its excellent viscosity, which makes it possible to mix the reagents homogeneously. In the process, glycol can provide reaction conditions adequate to greatly enhance solubility, diffusion, and crystallization, but is still mild to leave molecular building blocks to bring about the formation of the solid-state phase. At reaction temperature, the diffusion of ions in glycol is more rapid than in other polyol, such as glycerine and diethylene glycol; this leads to acceleration in the solubility of starting materials and in the following crystal growth. Both higher viscosity and lower viscosity are not beneficial for getting unique geometrical nanostructures. The concentrations of glycol of about 20–30 vol.%, were found to be favorable for the formation of the Cd(OH) $_2$ nanobelts in high yield. Such viscosity had a good effect on prohibiting aggregation of Cd(OH) $_2$ particles and then resulted in a relatively stable suspension. Control reactions at a low concentration of glycol (3 mL) would plate out a large amount of the Cd(OH) $_2$ nanorods (Fig. 5a). At very high concentrations

Fig. 2 XPS analysis of the nanobelts

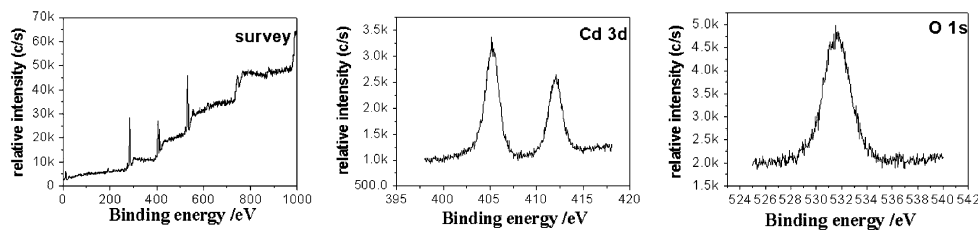


Fig. 3 Typical FESEM morphologies of the as-synthesized product. (a) Low-magnification image revealing large quantities of $\text{Cd}(\text{OH})_2$ nanobelts. (b) High-magnification image of curved nanobelts

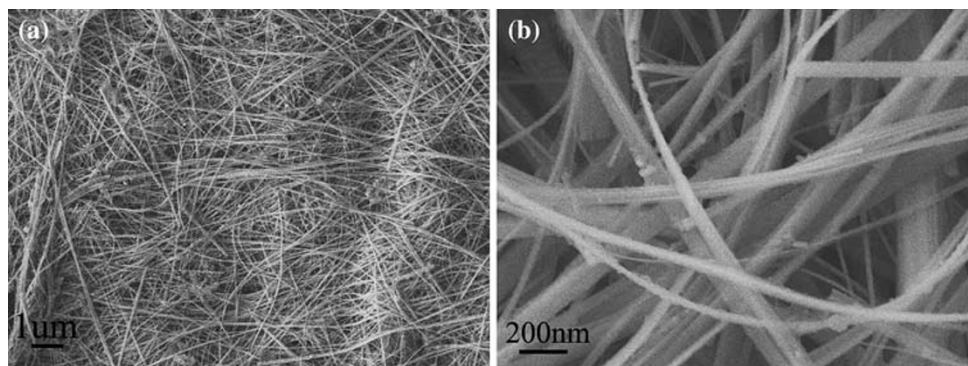
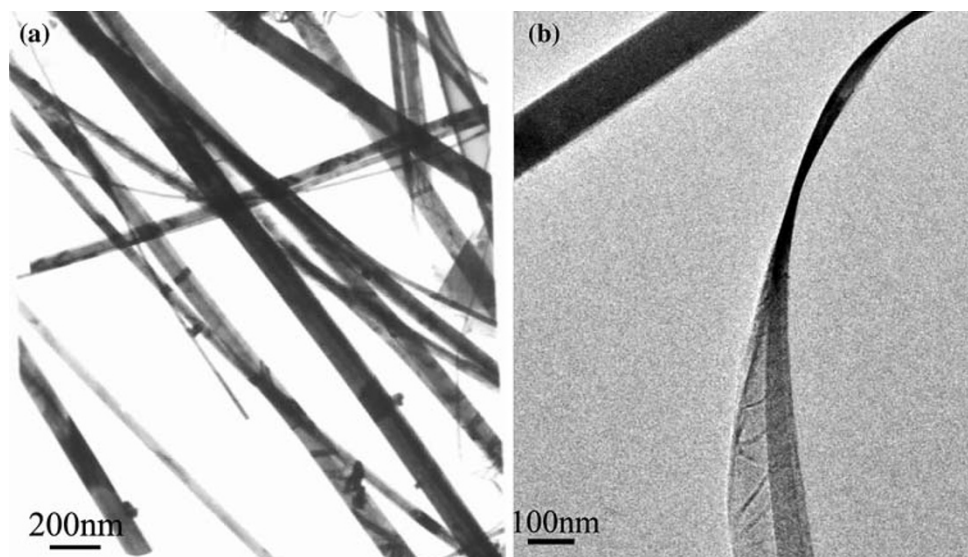


Fig. 4 TEM images of $\text{Cd}(\text{OH})_2$ nanobelts. (a) Regular $\text{Cd}(\text{OH})_2$ nanobelts. (b) Single curved $\text{Cd}(\text{OH})_2$ nanobelt



(20 mL glycol), however, only the aggregated particles were observed (Fig. 5b). Different solvents were also tested to reveal the solvent effect. When glycerine was used, nanobelts were not obtained due to the high viscosity of solvent. Usage of other polyol leads to similar results. From the experimental results, we can clearly see that the viscosity is of importance to the structure of the final product. The best solvent to get uniform belt-like pattern is glycol.

The optical absorption spectrum of our sample is shown in Fig. 6. Compared to other researcher's work [26], the absorption edge obviously shifts toward shorter

wavelength, i.e., blue shift. The absorption band gap E_g can be determined by the following equation: $(\alpha h\nu)^n = B(h\nu - E_g)$ [31], in which $h\nu$ is the photo energy, α is the absorption coefficient, B is a constant relative to the material, and n is either 2 for a direct transition or 1/2 for an indirect transition. The $(\alpha h\nu)^2 \sim h\nu$ curve for the samples shown in Fig. 6 insert reveals that the band gap of the samples is about 4.45 eV, which is larger than the reported value for $\text{Cd}(\text{OH})_2$ thin film ($E_g = 2.75$ eV) [25], but is less than the reported value for nanostrands, which have a constant width of 1.9 nm ($E_g = 4.76$ eV) [28] due to the quantum size effect [32].

Fig. 5 SEM images of $\text{Cd}(\text{OH})_2$ samples using different concentrations of glycol: (a) 3 mL; (b) 20 mL

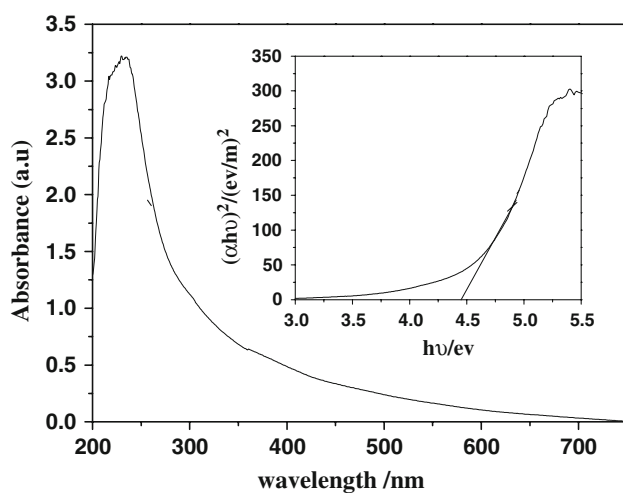
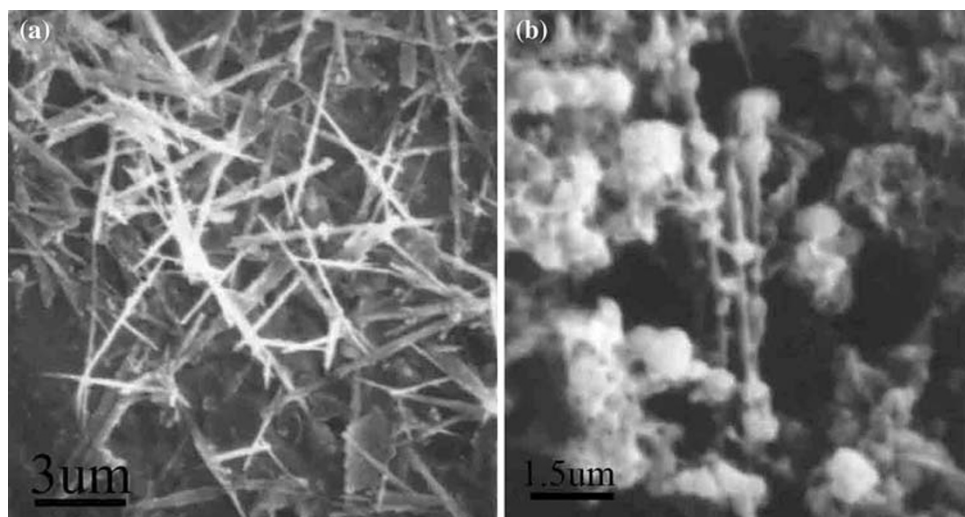


Fig. 6 Optical absorption spectrum and $(\alpha hv)^2 \sim hv$ curve for the $\text{Cd}(\text{OH})_2$ nanobelts

Conclusions

In summary, $\text{Cd}(\text{OH})_2$ nanobelts with a uniform diameter have been successfully prepared in high yield through a rapid polyol process. It was found that the viscosity of the solvent played an important role in determining the morphology. We believe that it should be possible to synthesize other similar patterns by choosing an appropriate solvent. The optical absorption spectrum indicates that the $\text{Cd}(\text{OH})_2$ nanobelts have a direct band gap of 4.45 eV.

Acknowledgment This work was supported by a Grant-in-aid for Scientific Research from the Japan Society for the Promotion of Science (JSPS) and the CREST program of the Japan Science and Technology Agency (JST). We are grateful to young and middle aged academic leaders of Jiangsu Province universities' "blue and green blue project." We are grateful to the electron microscope and X-ray diffraction facilities of university of science & technology of china for assistance in XRD and SEM measurement.

References

1. S. Frank, P. Poncharal, Z.L. Wang, W.A. de Heer, *Science* **280**, 1744 (1998)
2. X.F. Duan, C.M. Liber, *J. Am. Chem. Soc.* **122**, 188 (2000). doi:10.1021/ja993713u
3. Z.L. Wang, *Adv. Mater.* **12**, 1295 (2000). doi:10.1002/1521-4095(200009)12:17<1295::AID-ADMA1295>3.0.CO;2-B
4. Z.W. Pan, Z.R. Dai, Z.L. Wang, *Science* **291**, 2001 (1997)
5. L.H. Dong, Y. Chu, Y. Liu, M.Y. Li, F.Y. Yang, L.L. Li, *J. Coll. Inter. Sci.* **301**, 503 (2006). doi:10.1016/j.jcis.2006.05.027
6. A.Y. Rakovich, V. Stockhausena, A.S. Sushaa, S. Sapraa, A.L. Rogach, *Colloids Surf. A* **317**, 737 (2008). doi:10.1016/j.colsurfa.2007.12.010
7. Z.Z. Zhou, Y.L. Deng, *J. Coll. Inter. Sci.* **316**, 183 (2007). doi:10.1016/j.jcis.2007.07.038
8. Y.Y. Wu, H.Q. Yan, M. Huang, B. Messer, J.H. Song, P.D. Yang, *Chem Eur. J.* **8**, 1261 (2002)
9. Z.R. Dai, Z.W. Pan, Z.L. Wang, *Adv. Funct. Mater.* **13**, 9 (2003). doi:10.1002/adfm.200390013
10. C. Ma, D. Moore, J. Li, Z.L. Wang, *Adv. Mater.* **15**, 228 (2003). doi:10.1002/adma.200390052
11. Y. Jiang, X.M. Meng, J. Liu, Z. Xie, Y. Lee, S.T. Lee, *Adv. Mater.* **15**, 323 (2003). doi:10.1002/adma.200390079
12. J. Gong, S. Yang, J. Duan, R. Zhang, Y. Du, *Chem. Commun. (Camb)*. **351** (2005). doi:10.1039/b412289e
13. C.M. Liddell, C.J. Summers, *J. Coll. Inter. Sci.* **274**, 103 (2004). doi:10.1016/j.jcis.2003.12.012
14. T. Jong, D.L. Parry, *J. Coll. Inter. Sci.* **275**, 61 (2004). doi:10.1016/j.jcis.2004.01.046
15. M. Yekeler, H. Yekeler, *J. Coll. Inter. Sci.* **284**, 694 (2005). doi:10.1016/j.jcis.2004.10.046
16. P.H. Borse, W. Vogel, S.K. Kulkarni, *J. Coll. Inter. Sci.* **293**, 437 (2006). doi:10.1016/j.jcis.2005.06.056
17. P. Chiriță, M. Descostes, *J. Coll. Inter. Sci.* **294**, 376 (2006). doi:10.1016/j.jcis.2005.07.047
18. B. Tang, L.H. Zhuo, J.C. Ge, J.Y. Niu, Z.Q. Shi, *Inorg. Chem.* **44**, 2568 (2005). doi:10.1021/ic049195s
19. Z.A. Peng, X. Peng, *J. Am. Chem. Soc.* **123**, 1389 (2001). doi:10.1021/ja0027766
20. Z.A. Peng, X. Peng, *J. Am. Chem. Soc.* **124**, 3343 (2002). doi:10.1021/ja0173167
21. X. Wang, Y.D. Li, *Chem. Eur. J.* **9**, 5627 (2003). doi:10.1002/chem.200304785

22. H.W. Liao, Y.F. Wang, X.M. Liu, Y.D. Li, Y.T. Qian, *Chem. Mater.* **12**, 2819 (2000). doi:[10.1021/cm000096w](https://doi.org/10.1021/cm000096w)
23. G.R. Patzke, A. Michailovski, F. Krumeich, R. Nesper, J.D. Grunwaldt, A. Baiker, *Chem. Mater.* **16**, 1126 (2004). doi:[10.1021/cm031057y](https://doi.org/10.1021/cm031057y)
24. A.W. Xu, Y.P. Fang, L.P. You, H.Q. Liu, *J. Am. Chem. Soc.* **125**, 1494 (2003). doi:[10.1021/ja029181q](https://doi.org/10.1021/ja029181q)
25. H. Zhang, X.Y. Ma, Y.J. Ji, J. Xu, D.R. Yang, *Mater. Lett.* **59**, 56 (2005). doi:[10.1016/j.matlet.2004.08.027](https://doi.org/10.1016/j.matlet.2004.08.027)
26. M. Ristic, S. Popovic, S. Music, *Mater. Lett.* **58**, 2494 (2004). doi:[10.1016/j.matlet.2004.03.016](https://doi.org/10.1016/j.matlet.2004.03.016)
27. R.S. Mane, S.-H. Han, *Electrochem. Commun.* **7**, 205 (2005). doi:[10.1016/j.elecom.2004.12.010](https://doi.org/10.1016/j.elecom.2004.12.010)
28. Y.H. Luo, J.G. Huang, I. Ichinose, *J. Am. Chem. Soc.* **9**, 8297 (2005)
29. C.D. Wager, W.M. Riggs, L.E. Davis, J.F. Moulder, G.E. Muilenberg, *Handbook of X-Ray Photoelectron Spectroscopy*, Perkin-Elmer Corporation. Physical Electronics Division, Eden Prairie Minn., 55344 (1979)
30. J.S. Hammaond, S.W. Gaarenstroom, N. Winograd, *Anal. Chem.* **47**, 2194 (1975)
31. J.I. Pankove, *Optical processes in semiconductors* (Prentice-Hall, Englewood Cliffs, NJ, 1971)
32. X.H. Liao, J.H. Zhu, J.J. Zhu, J.Z. Xu, H.Y. Chen, *Chem. Commun. (Camb)* **937** (2001). doi:[10.1039/b101004m](https://doi.org/10.1039/b101004m)